Large horizontal gradients in atmospheric CO at the synoptic scale as seen by spaceborne Measurements of Pollution in the Troposphere

J. Liu,[1] J. R. Drummond,[1] D. B. A. Jones,[1] Z. Cao,[2] H. Bremer,[1,3] J. Kar,[1] J. Zou,[1] F. Nichitiu,[1] and J. C. Gille[4]

Received 13 April 2005; revised 24 August 2005; accepted 4 November 2005; published 25 January 2006.

[1] We have examined the influence of synoptic processes on the distribution of atmospheric CO as observed by the Measurements of Pollution in the Troposphere (MOPITT) satellite instrument. In the MOPITT data, large horizontal gradients in CO, coherent at the synoptic scale, have been observed. The concentration of CO varies rapidly by as much as 50–100% across distances of ~100 km, forming distinct boundaries in the CO distribution. These can last one to several days and span horizontal distances of 600–1000 km. On average, such events were observed in the MOPITT CO daily images once every 3–4 days over North America in spring and summer 2000. We focused on three case studies over North America in August 2000 to understand the mechanisms responsible for the large gradients in CO. Through an analysis of meteorological data from the National Centers for Environmental Prediction/National Center for Atmospheric Research Reanalysis, parcel trajectory modeling, and global three-dimensional chemical transport modeling, we found that the large horizontal gradients typically reflect the differential vertical and horizontal transport of air with different chemical signatures. In the first case, the large gradients in CO over North Dakota resulted from the lifting ahead of a cold front that transported boundary layer air enriched with CO from forest fires in Montana, combined with the descent of clean air from the Canadian Prairies behind the front. In the second case, the large gradients over northeastern Texas were produced by the convective lifting over Arkansas of air with high concentrations of CO from the oxidation of volatile organic compounds and the onshore transport of clean air from the Gulf of Mexico. In the third case, we examined an example of outflow of surface pollution from North America by a cyclone. The largest gradients in this case were observed along the boundary between the boundary layer air transported by the warm conveyor belt ahead of the cold front and the clean air transported from the Atlantic by the semipermanent high-pressure system in the central Atlantic. Our results demonstrate that MOPITT can capture the influence of synoptic processes on the horizontal and vertical distribution of CO. The large gradients in CO observed on synoptic scales represent valuable information that can be exploited to improve our understanding of atmospheric CO. In particular, these results suggest that the MOPITT observations provide a useful data set with which to address a range of issues from air quality on local/regional scales to long-range transport of pollution on continental/global scales.

Citation: Liu, J., J. R. Drummond, D. B. A. Jones, Z. Cao, H. Bremer, J. Kar, J. Zou, F. Nichitiu, and J. C. Gille (2006), Large horizontal gradients in atmospheric CO at the synoptic scale as seen by spaceborne Measurements of Pollution in the Troposphere, *J. Geophys. Res.*, *111*, D02306, doi:10.1029/2005JD006076.

1. Introduction

[2] Carbon monoxide (CO) is an important trace gas in the atmosphere. It is a major precursor of tropospheric ozone and is the principal sink for the hydroxyl radical (OH), the primary oxidant in the atmosphere. CO has a lifetime of weeks to months and its distribution is highly variable, reflecting the influences of a range of atmospheric transport processes. In particular, synoptic disturbances, which generally have spatial scales of hundreds of kilometers to thousands of kilometers and timescales from

[1]Department of Physics, University of Toronto, Toronto, Ontario, Canada.
[2]Meteorological Service of Canada–Ontario, Burlington, Ontario, Canada.
[3]Now at Institute of Environmental Physics, University of Bremen, Bremen, Germany.
[4]National Center for Atmospheric Research, Boulder, Colorado, USA.

0148-0227/06/2005JD006076$09.00

hours to days [*Daley*, 1991], are a significant source of its variability in the troposphere.

[3] *Brown et al.* [1984] and *Banic et al.* [1986] were among the first to observe large changes in the abundance of atmospheric pollutants associated with the passage of frontal systems. *Chung et al.* [1999] found episodes of high CO associated with certain synoptic processes over Hong Kong. Similarly, *Wang et al.* [2003] reported rapid changes in the abundance of air pollutants, such as CO and O_3, during the passages of cold fronts. *Fischer et al.* [2002] noticed sharp gradients in trace gas concentrations along a cold front. On the basis of the analysis of aircraft observations and modeling studies, it is now widely recognized that frontal lifting is an important pathway for the export of pollution from the boundary layer to the free troposphere [e.g., *Bethan et al.*, 1998; *Stohl*, 2001; *Donnell et al.*, 2001; *Kowol-Santen et al.*, 2001; *Heald et al.*, 2003; *Liu et al.*, 2003; *Chan et al.*, 2004; *Li et al.*, 2005].

[4] Continuous regional and global observations of the spatial variations in atmospheric CO became possible when the Measurements of Pollution in the Troposphere (MOPITT) began making measurements of CO from space in 2000. Large horizontal gradients in the distribution of CO at the synoptic scale have been observed in the MOPITT data. These variations in CO can be as large as 50–100% and occur over spatial scales of ~100 km. These events usually last one to several days, can span horizontal distances of 600–1000 km, and can appear over a range of pressure levels from 850 to 150 hPa. In this study, we use the MOPITT data at a resolution that is close to their native spatial and temporal resolution to examine the influence of synoptic process on the distribution of CO. In particular, we are interested in understanding the formation mechanisms responsible for the large horizontal gradients in CO at the synoptic scale observed in the MOPITT data.

[5] We examine three cases over North America in summer 2000. In the first case, we investigate a region of large horizontal gradients in CO over North Dakota, which was associated with a cold front. In the second case, we examine the influence of weather conditions near the northeast border of Texas on the distribution of CO. In the third case, we focus on the export of CO from North America over the western Atlantic due to the passage of cyclone from the Great Lakes region to eastern Canada. To diagnose the mechanisms responsible for the observed CO distribution, we combine parcel trajectory and chemical transport modeling together with analysis of meteorological data from the National Centers for Environmental Prediction/National Center for Atmospheric Research (NCEP/NCAR) Reanalysis.

2. Data and Analysis Method

2.1. MOPITT and NCEP Data

[6] The CO data are from the MOPITT instrument [*Drummond*, 1992] aboard the Terra satellite. The spacecraft is flying in a sun synchronous polar orbit at an altitude of 705 km. It makes 14–15 daytime and nighttime passes per day, crossing the equator around 1045 and 2245 local time. MOPITT uses a cross-track scanning method with a swath of ~600 km, consisting of 29 pixels per swath with a horizontal resolution of 22 × 22 km^2 per pixel. It achieves near-complete global coverage in 3 days.

[7] MOPITT measures upwelling infrared radiation from which vertical profiles of atmospheric CO are retrieved. The retrieval algorithm employs a maximum likelihood optimal estimation technique, the maximum a posteriori solution (MAP) [*Rodgers*, 2000], which has been described in detail in previous studies [*Pan et al.*, 1998; *Edwards et al.*, 1999; *Deeter et al.*, 2003]. In the retrieval, pixels with thick clouds are screened out with the algorithms developed by *Warner et al.* [2001]. The MOPITT data consist of profiles of CO, reported on 7 pressure levels (surface, 850, 700, 500, 350, 250, and 150 hPa), and the total column abundance of CO. The vertical sensitivity of the MOPITT retrievals indicates that the MOPITT profile data are highly correlated with about 1–2 pieces of independent vertical information in each sounding. Since the instrument measures infrared emissions, it has low sensitivity to the CO in the boundary layer. This can be further explained as follows. In the MOPITT retrieval algorithm, the retrieved CO profiles ($\hat{x}$) are expressed approximately as a weighted average of the "true" profiles (x) and the a priori profile (x_a):

$$\hat{x} \approx Ax + (I - A)x_a \tag{1}$$

where I is the identity matrix and A is the averaging kernel matrix. The averaging kernels are determined by the a priori error covariance and the retrieval error covariance and are provided for each MOPITT CO profile. The averaging kernels indicate the sensitivity of the retrieved CO at one pressure level to the CO at other levels. In the ideal case, A would be equal to I, which means that the CO retrieval at a pressure level is only sensitive to the CO variation at that level. As a result, in this case, the retrieved profiles would represent the true profiles. In the worst case, A would be zero and the retrieved CO profiles are equal to the a priori, meaning the variation in CO profiles from the a priori cannot be captured. In reality, A is less than I. An analysis of the degrees of freedom of signal [*Deeter et al.*, 2004] shows that MOPITT data can distinguish the middle troposphere (500–700 hPa) and the upper troposphere (200–300 hPa). The averaging kernels have a low value near the surface, indicating that MOPITT is insensitive to CO at the surface and therefore the surface values are not used in this study. The lowest level used is the 850 hPa level where the values of the averaging kernels are higher than near the surface [*Deeter et al.*, 2004; *Emmons et al.*, 2004]. The sensitivity of MOPITT to CO usually increases with altitude from the surface to 850 hPa.

[8] Extensive validation of the MOPITT CO data has been performed by *Emmons et al.* [2004], using a variety of in situ aircraft data. *Emmons et al.* [2004] found that for March 2000 to May 2001, the bias in the MOPITT data was less than 20 ppbv for profile data and 5 ± 11% for total CO column observations. In the analysis presented in this study, the satellite track data were averaged on a 0.25° × 0.25° grid, which, at 40°N, is similar in resolution to the MOPITT footprint. The MOPITT data are available from NASA Langley Atmospheric Science Data Center at http://eosweb.larc.nasa.gov/PRODOCS/mopitt/table_mopitt.html.

[9] To diagnose the air motion associated with the observed CO distribution, we use the horizontal wind (u and v)

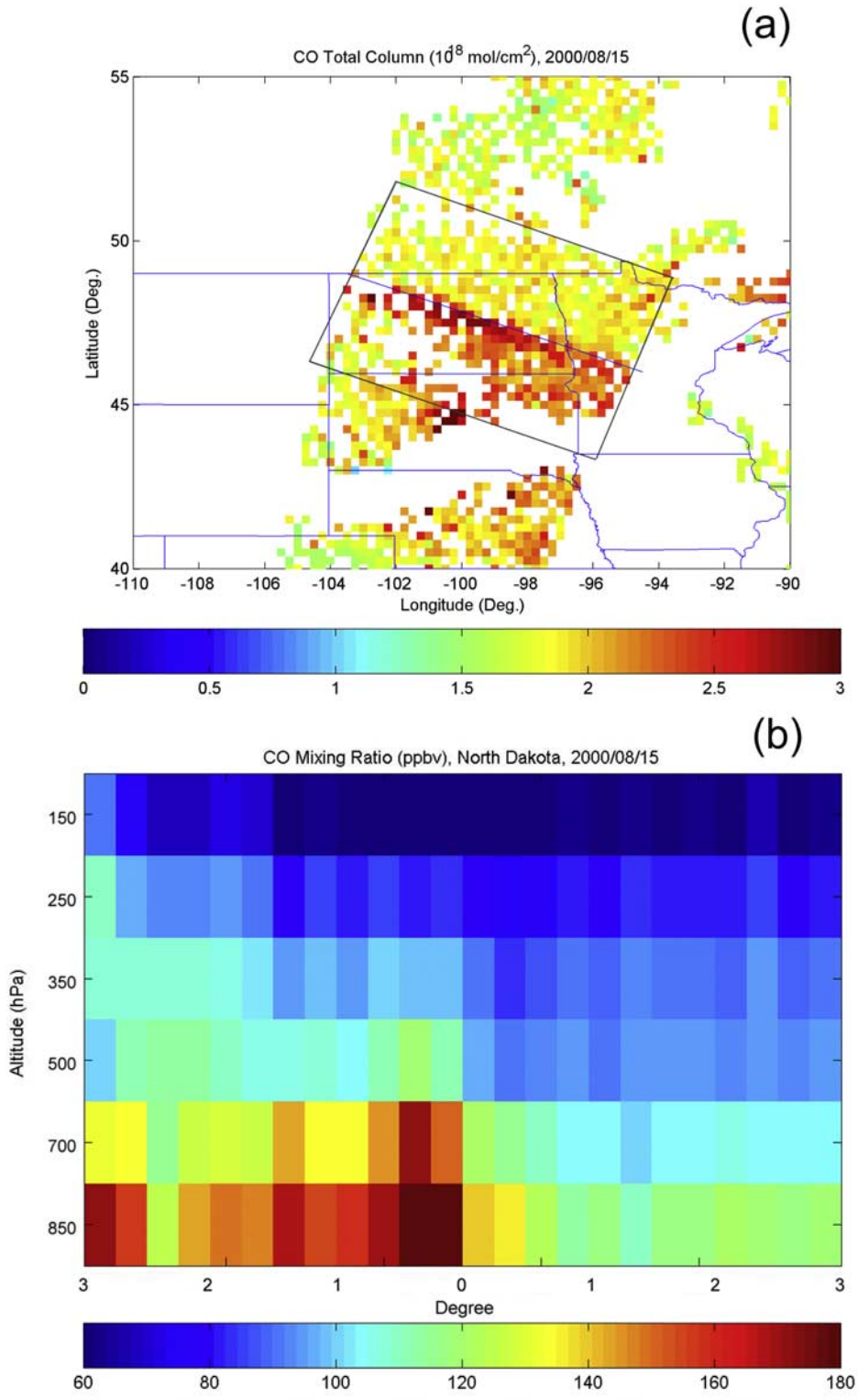

Figure 1. (a) CO total column (in 10^{18} molecules cm^{-2}) over North Dakota in the United States on 15 August 2000. The location of the largest CO gradient is indicated with a line, which is used in other figures as a location reference. State boundaries are also outlined. MOPITT overpass time was around 1800 UTC (1200 local time). (b) Vertical cross section of the CO distribution. The cross section is normal to the reference line in Figure 1a, extending ±3 degrees (=12 pixels) from the reference line to each side. The mixing ratio values (in ppbv) represent the mean value within the boxed area in Figure 1a, averaged along the direction parallel to the reference line. Note that the vertical axis indicates the pressure levels for the MOPITT retrievals that are not evenly spaced. The surface CO is excluded because of low sensitivity of MOPITT to the CO in the boundary layer.

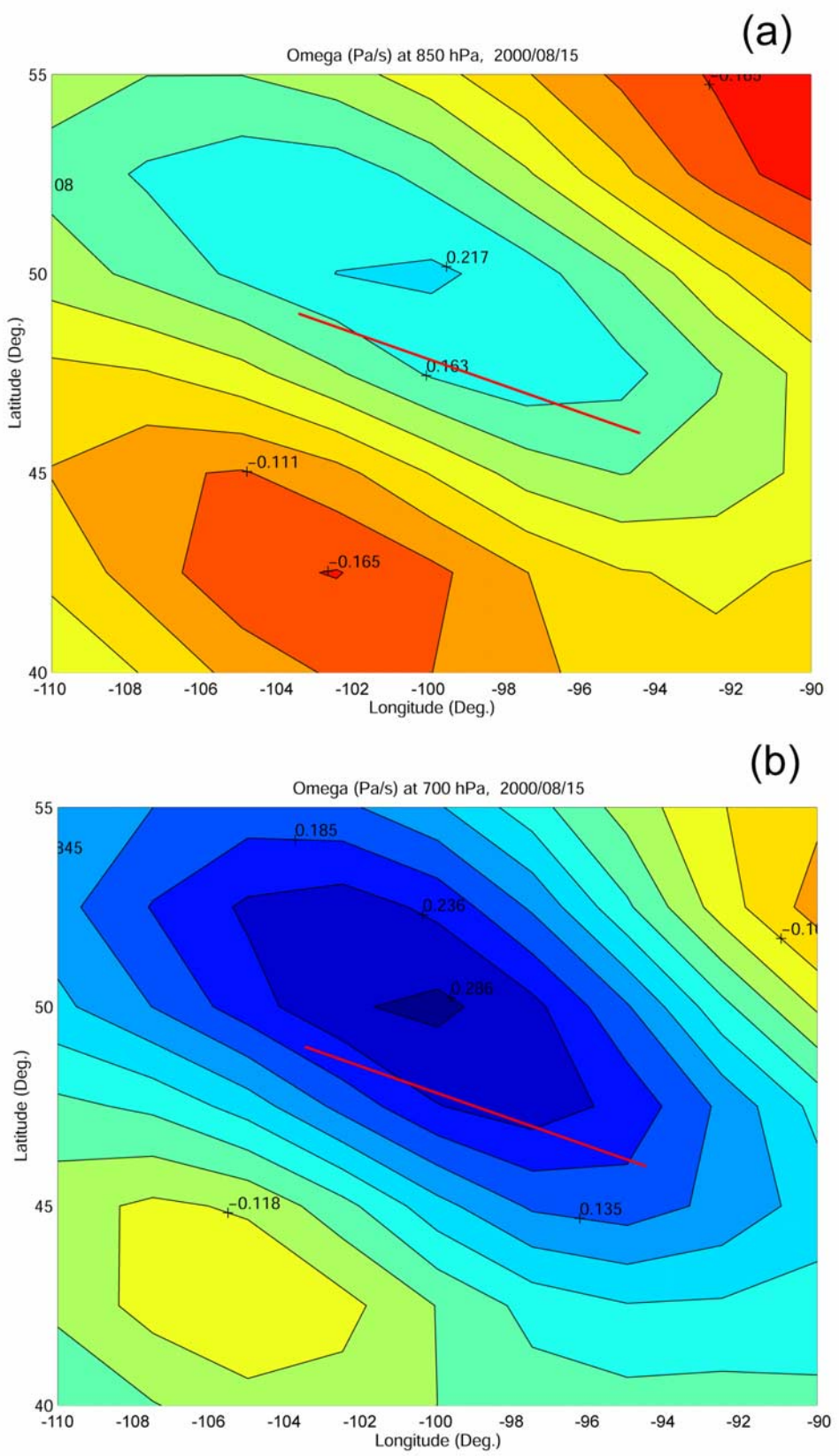

Figure 2. Daily mean vertical motions on 15 August 2000 as inferred from the pressure tendency ($\omega = dp/dt$, in Pa s^{-1}) at (a) 850 hPa and (b) 700 hPa in the NCEP Reanalysis data. Upward motion ($\omega < 0$) is indicated by red and yellow, and downward motion ($\omega > 0$) is indicated by blue. The straight line indicates the location of the reference line in Figure 1a.

and the vertical pressure tendency (ω) data from the NCEP Reanalysis data sets (http://www.cdc.noaa.gov/cdc/reanalysis/reanalysis.shtml). These data have a horizontal resolution of 2.5° and are available at several heights, including 1000, 850, 700, 500, 400, 250, and 150 hPa. We also obtained relevant air temperature, geopotential height, specific humidity, and relative humidity data from the reanalysis database.

2.2. Model Description

[10] The GEOS-CHEM model is a global three-dimensional chemical transport model driven by assimilated meteorological observations from the NASA Goddard Earth Observing System (GEOS-3). A detailed description of the first generation of the model, along with a comparison of model results with observations, is presented by *Bey et al.* [2001]. Recent updates and applications of the model have been described in a range of studies [e.g., *Park et al.*, 2003; *Fiore et al.*, 2003; *Wang et al.*, 2004; *Suntharalingam et al.*, 2004]. The version of GEOS-CHEM employed here is version 6.02.05 (http://www-as.harvard.edu/chemistry/trop/geos/index.html). It has a horizontal resolution of 2° × 2.5° with 48 sigma levels in the vertical from the surface to 0.01 hPa. The budget of CO is based on the source inventory of *Duncan et al.* [2003] and *Yevich and Logan* [2003] for biomass burning and biofuel emissions, respectively. Fossil fuel emissions are from *Bey et al.* [2001]. For the simulations presented here we calculate the CO distribution using monthly mean abundances of OH archived from a full chemistry simulation of the model [*Evans and Jacob*, 2005].

3. Results and Discussion

3.1. North Dakota Case

[11] A strong horizontal gradient in the total column abundance of CO was observed on 15 August 2000 over North Dakota, during a MOPITT daytime pass (Figure 1a). The total column abundance of CO increased rapidly from $\sim 1.7 \times 10^{18}$ molecules cm^{-2} to $\sim 3.0 \times 10^{18}$ molecules cm^{-2} across a distance of less than 100 km, forming a distinct boundary in the CO distribution. This boundary at least extended from 46°N, 94.5°W to 49°N, 103.5°W, across the entire MOPITT swath, but it is probably longer than the swath width of ~600 km. The vertical structure of the CO distribution perpendicular to the boundary is displayed in Figure 1b. The largest horizontal CO gradient, ~1.0 ppbv km^{-1}, was in the lower troposphere at 850 hPa, with much of the variation in CO across the boundary confined to the lower troposphere.

[12] Analysis of vertical motions (i.e., the pressure tendency, ω = dp/dt) in the NCEP Reanalysis data indicates that the high CO column abundances on the southern side of the boundary were associated with ascending airflow, suggesting the vertical transport of polluted air from the planetary boundary layer (Figure 2). In contrast, the descending airflow to the north of the boundary appears to be transporting clean air (low CO) down from the upper troposphere. The boundary was almost aligned with the transition between regions of subsidence and ascent in the lower troposphere at 850 hPa, but shifted slightly at higher pressure levels (e.g., 700 hPa).

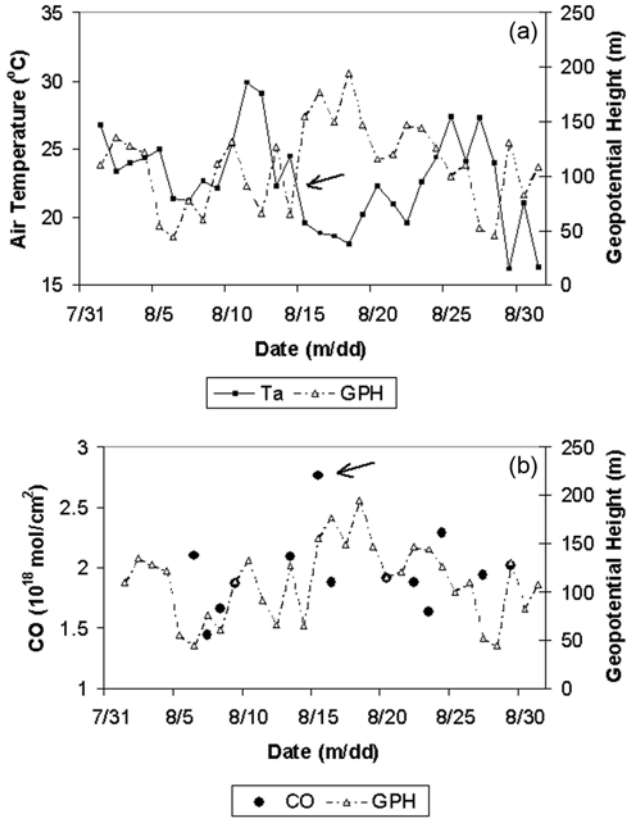

Figure 3. (a) Time series of daily mean air temperature (T_a in °C) and geopotential height (GPH, in meters) at 1000 hPa near the middle point of the reference line in Figure 1a for August 2000. (b) Time series of CO total column (in 10^{18} molecules cm^{-2}) at location 48°N, 101.5°W (near the reference line in Figure 1a on the higher-CO side, the mean of 4 pixels), and the corresponding geopotential height. The daytime MOPITT overpasses include 6, 8, 13, 15, 22, 24, 27, and 29 August. The rest are nighttime overpasses. The arrows indicate a rapid increase in CO total column and the passage of a cold front on 15 August 2000.

[13] The transition in vertical air motion was very likely associated with a cold front. We averaged the temperatures and geopotential heights from the NCEP Reanalysis data at 3 points near the middle of the reference line (48.3°N, 98.3°W) and found a rapid drop in air temperature and an increase in geopotential height at 1000 hPa on 15 August 2000, suggesting the passage of a cold front (Figure 3a). The surface observation data (Environment Canada, http://gfx.weatheroffice.ec.gc.ca/charts/index_e.html) reveal a large temperature difference of ~6°C between the two sides of the reference line and suggest that the reference line was very likely aligned with the cold front, with high CO ahead of the cold front and low CO behind the front. In comparing the timing of the passage of the cold front (Figure 3b), we found a jump of CO total column from $\sim 2.0 \times 10^{18}$ molecules cm^{-2} to 2.7×10^{18} molecules cm^{-2} on 15 August, taking the mean of 4 pixels at a location near the reference line at Figure 1a on the higher-CO side (48°N, 101.5°W).

[14] The sharp gradient in CO at this location was not seen during the following days of MOPITT overpasses after

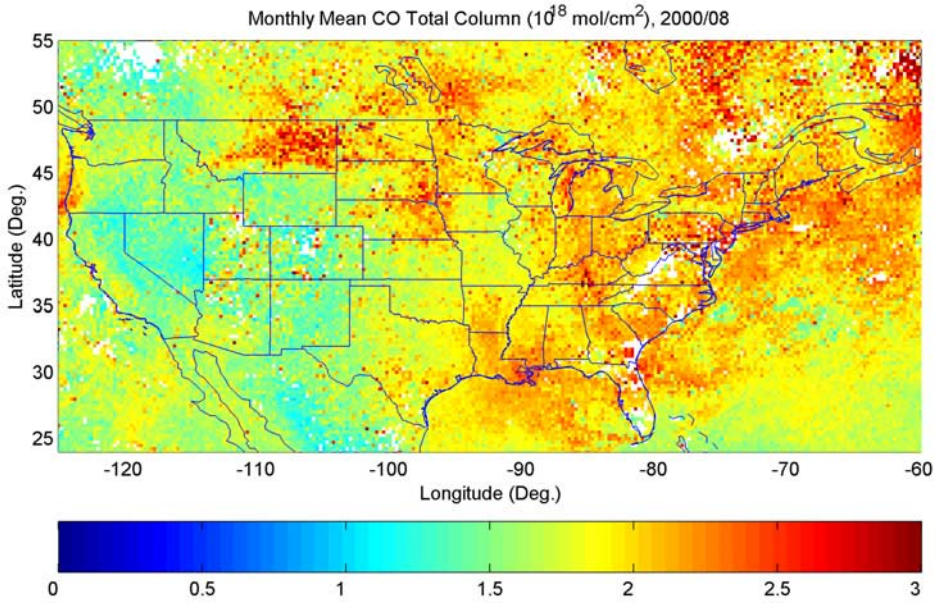

Figure 4. Monthly mean CO total column (in 10^{18} molecules cm^{-2}) over part of North America (24°–55°N, 60°–125°W). Note the high CO values in the state of Montana, where large fire events occurred in August 2000. The dashed line indicates the location of the reference line in Figure 1a.

the passage of the weather system. The sharp gradient is also not present in the monthly image of total column CO, shown in Figure 4. High concentrations of CO, however, were observed in much of the region, in particular eastern Montana (45°–50°N, 104°–110°W), due to biomass burning. Large fires were detected near the borders of Idaho, Montana, and Wyoming in August 2000, including 14 August [*Lamarque et al.*, 2003; *Liu et al.*, 2005]. Attempts to simulate the CO gradient in the GEOS-CHEM model failed because the biomass burning climatology in the model did not capture these fires.

[15] We performed a back trajectory analysis of the air masses over North Dakota using the Real-Time Environment Applications and Display System (READY) program at the NOAA Air Resources Laboratory (http://www.arl.noaa.gov/ready.html). A 24-hour back trajectory starting at 1.5 km (~850 hPa) on 15 August 2000 at 1800 UTC (1200 local time) over North Dakota suggests that the air parcels with high CO originated from Montana and were likely associated with the biomass burning plume (Figure 5a). In contrast, the trajectory analysis indicates that the air with low concentrations of CO north of the boundary came from the Canadian prairies, from a higher altitude of about 3.5 km (~600 hPa) (Figure 5b). The altitude of the southern trajectory varied by a much smaller amount than the northern one, remaining essentially at the same altitude for the previous 12 hours.

3.2. Texas Case

[16] MOPITT observations near Dallas, Texas, on 5 August 2000, reveal dramatic contrasts in the total column abundance of CO (Figure 6a). The total column CO rose from ~1.5×10^{18} molecules cm^{-2} to ~2.5×10^{18} molecules cm^{-2} within a distance of ~150 km, forming a distinct boundary in the CO distribution within a MOPITT daytime pass swath of ~600 km. The large CO gradient is also seen at all pressure levels from 850 hPa to 150 hPa (Figure 6b). The gradient was the largest at 850 hPa and the lowest at 150 hPa. Some pixels at 350 hPa had CO mixing ratios even larger than at 500 hPa, suggesting a deep convection process that was also observed by *Kar et al.* [2004]. The strong horizontal gradient in CO was not observed when MOPITT revisited the area on 7 August. Similar to the North Dakota case, the distinct boundary does not exist in the monthly mean CO image (Figure 4), suggesting that the CO distribution reflects the influences of synoptic weather processes.

[17] Analysis of the vertical motions in the NCEP data, shown in Figure 7, indicates that ascending motion was associated with high CO on the northern side of the boundary in the lower troposphere, while descending motion was linked to the low CO on the southern side. The reference line in Figure 6a appears to be aligned with the orientation of transition between the upward and downward motions with a slight shift toward the downward zone in the daily mean ω ($\omega = dp/dt$) field. The large areas with missing CO values due to clouds northeast of the reference line in Figure 6a also hint at possible upward motion. The location, season, and density of vertical flow appear to be in agreement with the findings of *Li et al.* [2005], who pointed out that this region is one of the areas in the United States where convection, which lifts surface pollution to the free troposphere, is very active in summer.

[18] To help interpret the MOPITT data, we use the GEOS-CHEM CTM to simulate the CO distribution observed by MOPITT over Texas. The modeled total column abundances of CO are shown in Figure 8a and are consistent with the observations. As a result of the coarse horizontal resolution of the model, however, the simulated CO gradient is less sharp than observed in the MOPITT data. Analysis of the modeled fields indicates that the dominant contribution to the horizontal gradient in the column data

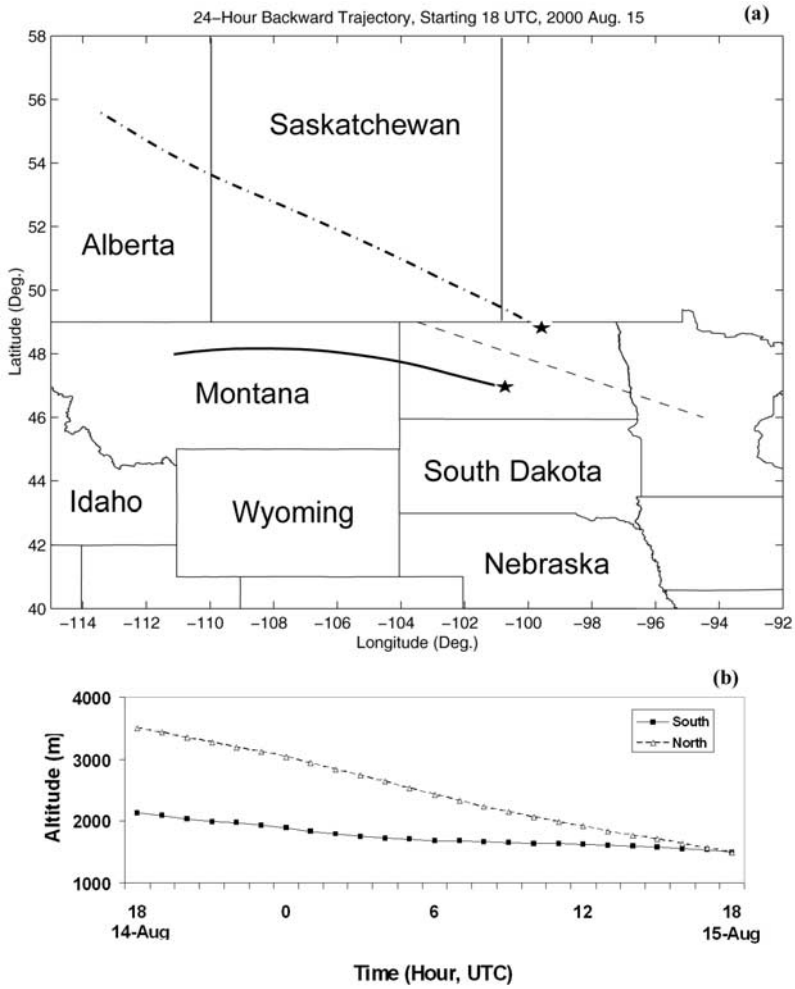

Figure 5. (a) Twenty-four-hour back trajectories starting at the locations marked with stars at 1.5 km altitude on 15 August at 1800 UTC (1200 local time). The dashed line indicates the location of the reference line in Figure 1a. The solid and dot-dashed lines trace trajectories from the high- and low-CO areas, respectively. The names of some states and provinces are indicated. (b) Time series of vertical motion for the same back trajectories in Figure 5a.

comes from the lower troposphere, and reflects the combined influence of the convective lifting of CO from a strong source over Arkansas and the transport of CO-poor air downward and poleward from the Gulf of Mexico. As a result of this vertical transport, the enhanced CO north of the boundary in the model (not shown) extends from the surface to the upper troposphere, in agreement with the vertical distribution of the MOPITT CO shown in Figure 6b. To better compare the model with the data, we sampled the model along the MOPITT orbit track and applied the averaging kernels. This smoothed representation of the model is shown in Figure 8b. Although MOPITT is not strongly sensitive to CO in the boundary layer, application of the averaging kernels generally does not destroy the gradients in the model, suggesting that differential vertical motions were an important criterion for the presence of the CO horizontal gradient in the MOPITT data. In this case, as well as in the other cases in this study, the CO gradients were associated with the lifting of polluted air masses into the free troposphere, where MOPITT was able to detect the CO signal.

[19] To identify the source of the enhanced CO observed by MOPITT, we performed a model simulation in which we "tagged" the CO from different North American sources, and found that the chemical production of CO from the oxidation of methane and volatile organic compounds (VOC) represents the dominant contribution to the enhancement in the CO column abundances. Figure 9 shows the CO produced from the oxidation of methane and VOCs. As the oxidation of methane provides a relatively uniform background source of CO, the local enhancement reflects primarily the effects of the VOC oxidation. This is consistent with previous studies [e.g., *Palmer et al.*, 2003; *Li et al.*, 2005] that have found that the oxidation of biogenic hydrocarbons is the dominant source of CO in the southern United States in summer. In the model, the enhanced CO over Arkansas on 5 August was associated with a plume of CO that originated over northern Louisiana and northeast Texas. The plume was transported northward in the boundary layer to the Arkansas region where it was convectively lifted to the free troposphere. By 7 August, after the passage of the synoptic system and the export of the plume from the

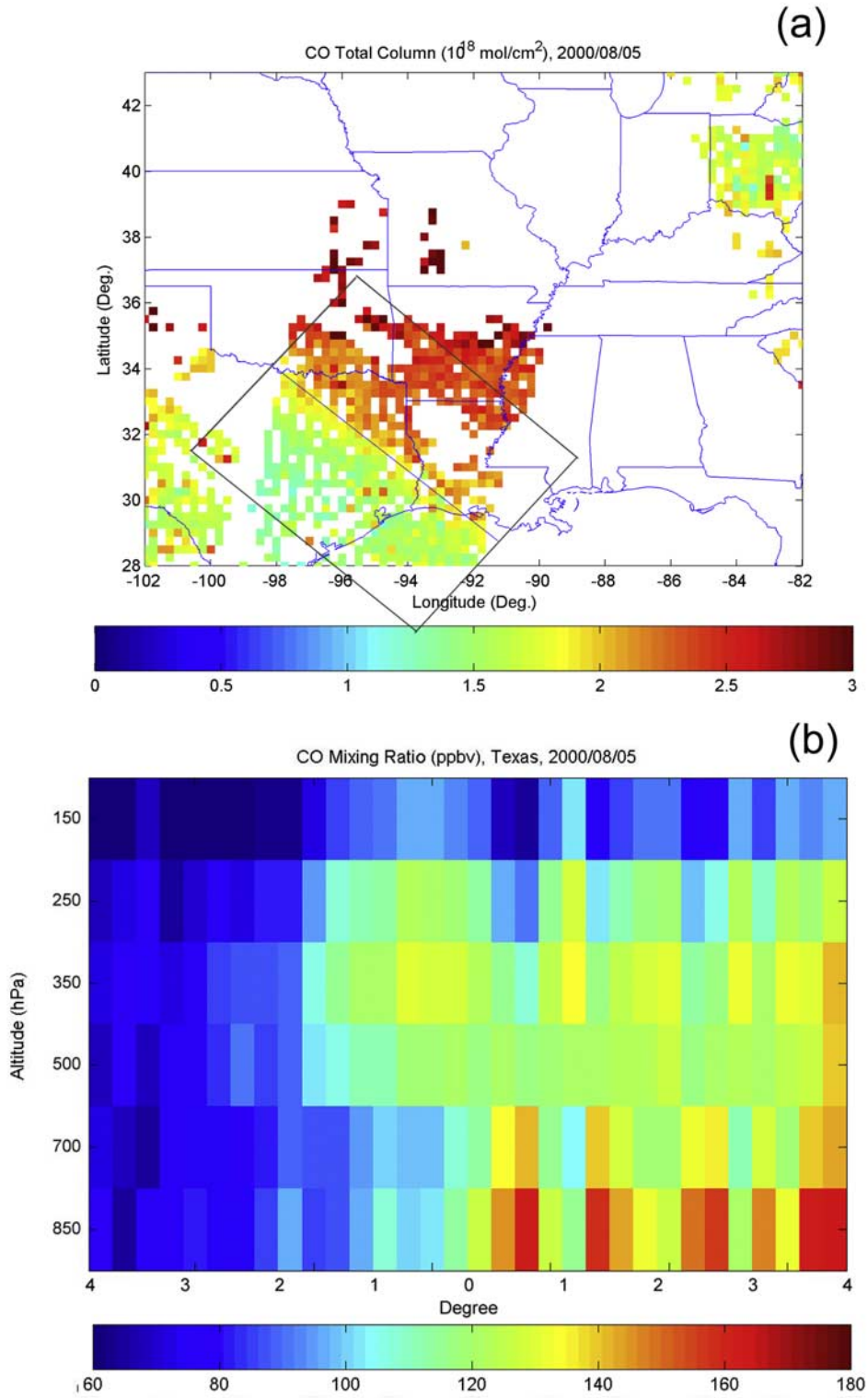

Figure 6. (a) CO total column (in 10^{18} molecules cm^{-2}) over Texas in the United States on 5 August 2000. The location of the largest CO gradient is indicated with a line, which is used in other figures as a location reference. (b) Vertical cross section of the CO distribution. The cross section is normal to the reference line in Figure 6a, extending ±4 degrees (=16 pixels) from the reference line to each side. The mixing ratio values (in ppbv) represent the mean value within the boxed area in Figure 6a, averaged along the direction parallel to the reference line. Note that the vertical axis indicates the pressure levels for the MOPITT retrievals that are not evenly spaced. The surface CO is excluded because of low sensitivity of MOPITT to the CO in the boundary layer.

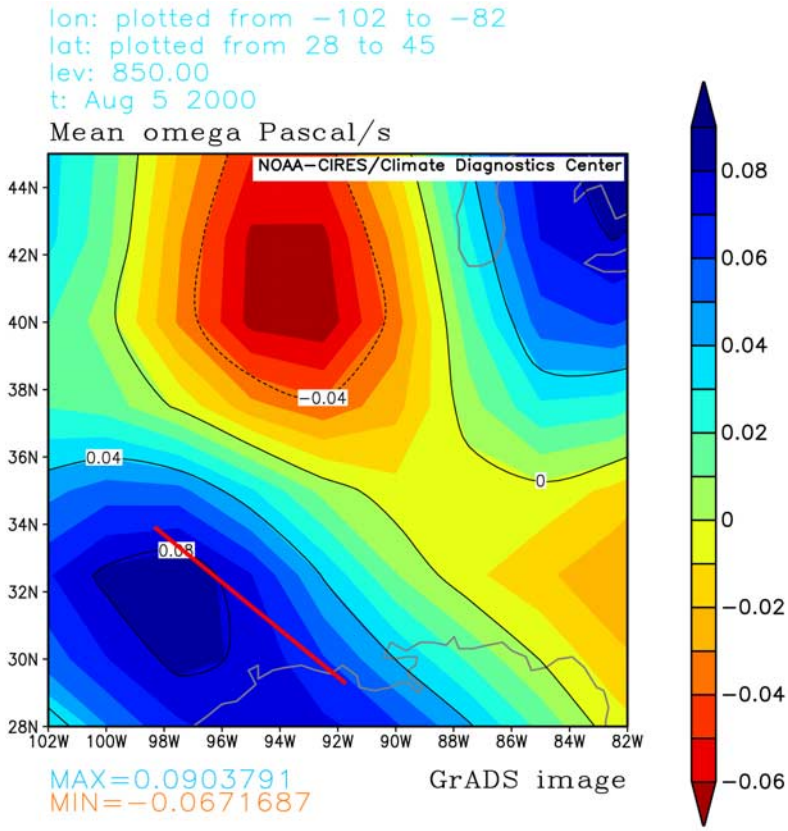

Figure 7. Daily mean vertical motion on 5 August at 850 hPa as inferred from the pressure tendency ($\omega = dp/dt$, in Pa s^{-1}) in the NCEP data. Upward motion ($\omega < 0$) is indicated by red, and downward motion ($\omega > 0$) is indicated by blue. The red line indicates the location of the reference line in Figure 6a.

boundary layer over Arkansas, the large gradients in CO over northeastern Texas were absent in both the model and the MOPITT data.

[20] Compared to the case in North Dakota, there is substantially more CO in the middle to upper troposphere (Figure 1b versus Figure 6b). This may be explained by the active convection in this region and the weather systems in the upper troposphere. *Li et al.* [2005] found that in summer there is usually a semipermanent anticyclone in the middle to upper troposphere over the southern United States that can recirculate lifted surface pollution around for days. This anticyclone is also found for the Texas case on 5 August 2000 (Figure 10a). In the North Dakota case, in contrast, the front-lifted surface CO was rapidly transported away in the upper troposphere by the predominantly westerly winds (Figure 10b), as also reported by *Li et al.* [2005]. This comparison of vertical CO distribution between the two cases provides new evidence of MOPITT's capability to observe CO vertical variations and the associated implications for CO transport.

3.3. Western Atlantic Case

[21] We focus here on the eastern coast of the United States. The large horizontal gradient in CO is seen in several MOPITT daytime and nighttime swaths spanning over 1000 km distance on 7 August 2000 (Figure 11a, daytime swath: from northeast to southwest; nighttime swath: from southeast to northwest). The vertical structure across a swath in a nighttime pass (the boxed area in Figure 11a) is showed in Figure 11b. In the northern region of the swath, enhanced abundances of CO occurred at all pressure levels. This phenomenon is also observed on 8 and 9 August 2000 (Figure 12).

[22] This is a case of the outflow of North American pollution, which was the subject of the International Consortium on Atmospheric Transport and Transformation (ICARTT) campaign in summer 2004 and several other studies [e.g., *Li et al.*, 2005]. Figure 13a shows an example of the weather system on 8 August 2000, using the geopotential height at 1000 hPa from NCEP Reanalysis data. The cyclone system over eastern Canada on 8 August 2000 originally developed over the Great Lakes region on 7 August. The system split into two on 9 August, one part moved eastward and the other stayed between the Great Lakes region and Newfoundland. There was a stable high-pressure system over the Atlantic Ocean on these days. The cyclone near Newfoundland and the anticyclone over the Atlantic Ocean can be seen in a GEOS satellite image on 8 August 2000 at 0000 UTC time (Figure 13b), with a cold front extending down along the North American coast, behind the band of clouds.

[23] The CO total columns simulated by the GEOS-CHEM model for 7 August 2000 are shown in Figure 14a. In both the model and observations, the highest abundance of CO was associated with the vertical transport of pollution from the northeastern United Stated by the warm conveyor belt (WCB)

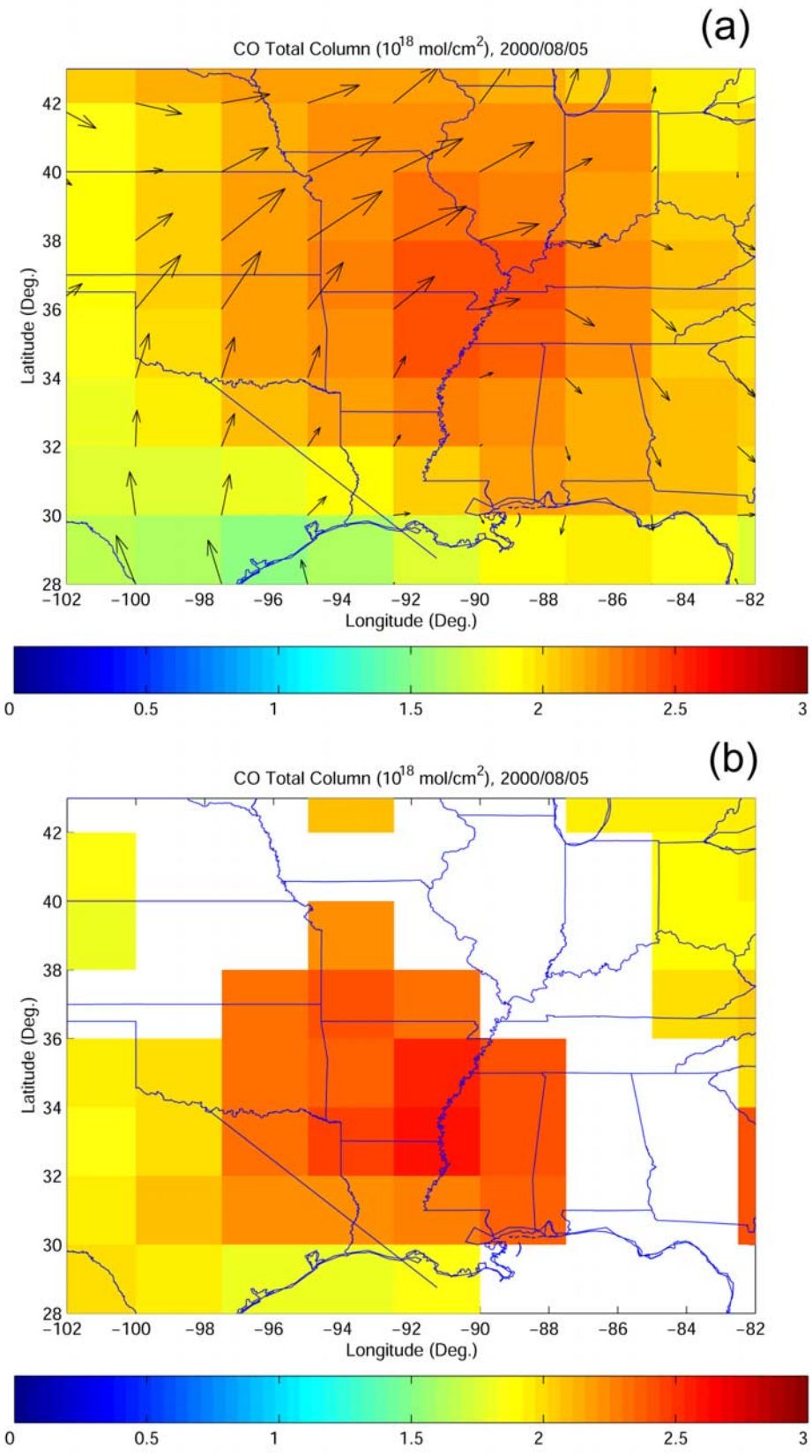

Figure 8. (a) Daily mean CO total column (in 10^{18} molecules cm^{-2}) on 5 August 2000 as simulated by the GEOS-CHEM model. The modeled winds at the 850 hPa level are overlaid as arrows. The mean wind speed over the image was 5.5 m s^{-1}. (b) Modeled CO fields in Figure 8a after application of the local MOPITT averaging kernels. White areas indicate missing values due to clouds. The straight line indicates the location of the reference line in Figure 6a.

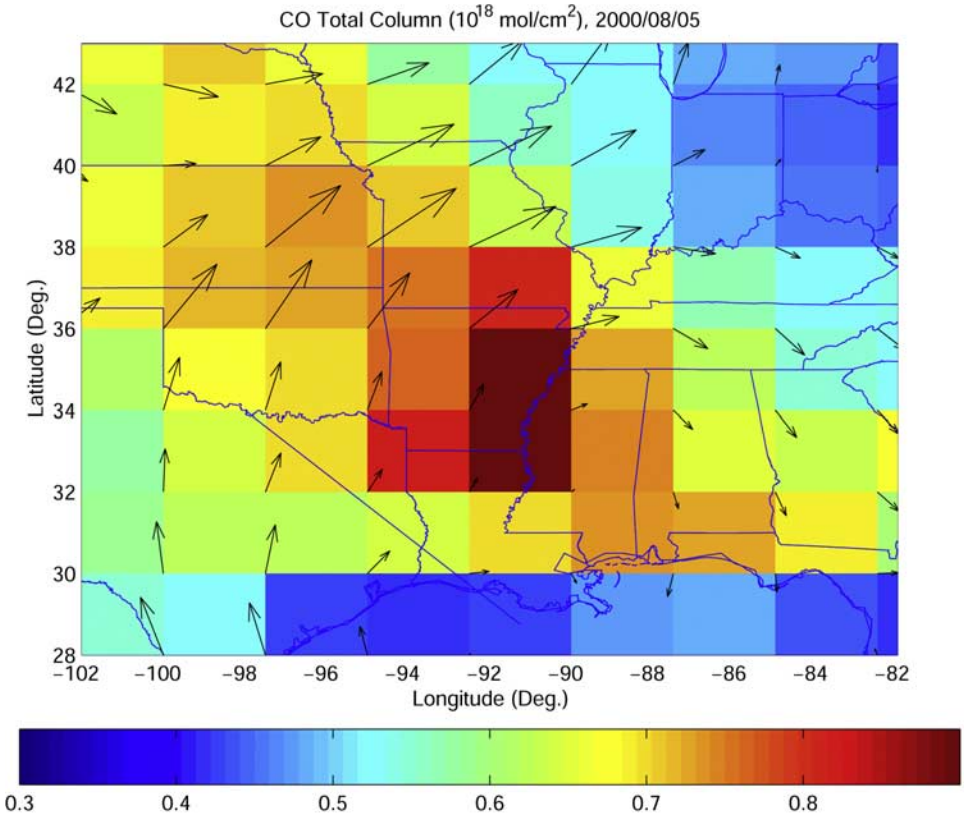

Figure 9. CO total column (in 10^{18} molecules cm^{-2}) produced from the oxidation of methane and volatile organic compounds in the GEOS-CHEM model for 5 August 2000. The modeled winds at the 850 hPa level are overlaid as arrows. The mean wind speed over the image was 5.5 m s^{-1}. The straight line indicates the location of the reference line in Figure 6a.

ahead of the cold front associated with the cyclone. In the MOPITT data (Figure 12), the largest gradients in CO are found along the boundary between the WCB and the clean air transported from the Atlantic Ocean by the high-pressure system in the central Atlantic. The distinct boundary between high and low CO was mostly aligned with a zone where the horizontal wind directions changed rapidly (wind shear) along the two sides of the high-pressure system. Therefore clear air was transported from ocean to land while the polluted air was blown in the opposite direction, which is further confirmed with trajectory analysis. The high-pressure system was relatively stable and persisted for several days. As a result, the large horizontal gradient of CO is observable in those days with little change in location. As the same for the Texas case (Figure 8b), the MOPITT local averaging kernels are applied to the GEOS-CHEM CO columns (Figure 14b). The location, orientation, and magnitude of the large horizontal gradient in CO are consistent with those in the modeled CO column fields after the application of the averaging kernels.

[24] The three cases illustrate that the large horizontal CO gradients were observable by MOPITT under certain conditions when air parcels on the opposite sides of the boundary retained substantial differences in CO content due to strong CO sources on one side and shifts in the local wind directions. On average, those large horizontal gradients appeared on the MOPITT daily CO images once per 3–4 days over North America (20°–85°N, 50°–175°W) from May to September 2000. There were more such cases in summer than in autumn (in October, the frequency reduced to once per 10 days). In some cases, these gradients were smaller than the three cases shown in this study. Similar cases were also observed in other continents. An example was on 24 August 2000 over northeast of China (40°N, 120°E) (not shown).

3.4. Suggestions for Application of MOPITT Data in Future Studies

[25] Earlier work has shown that the MOPITT CO can be reliably used to study deep convection, particularly in the tropics [*Deeter et al.*, 2004; *Kar et al.*, 2004]. This work shows that convective signatures in CO data are still present at the mid latitudes despite somewhat lower vertical resolutions at these latitudes than in the tropics. In addition, lifting in the WCB was seen clearly in the CO data. From an examination of MOPITT CO images, it was found that sharp synoptic-scale CO gradients occurred frequently over North America. In future work, this analysis can be extended to other continents. Given that the MOPITT data now cover more than 5 years, this represents an unprecedented opportunity to carry out global statistical studies of CO

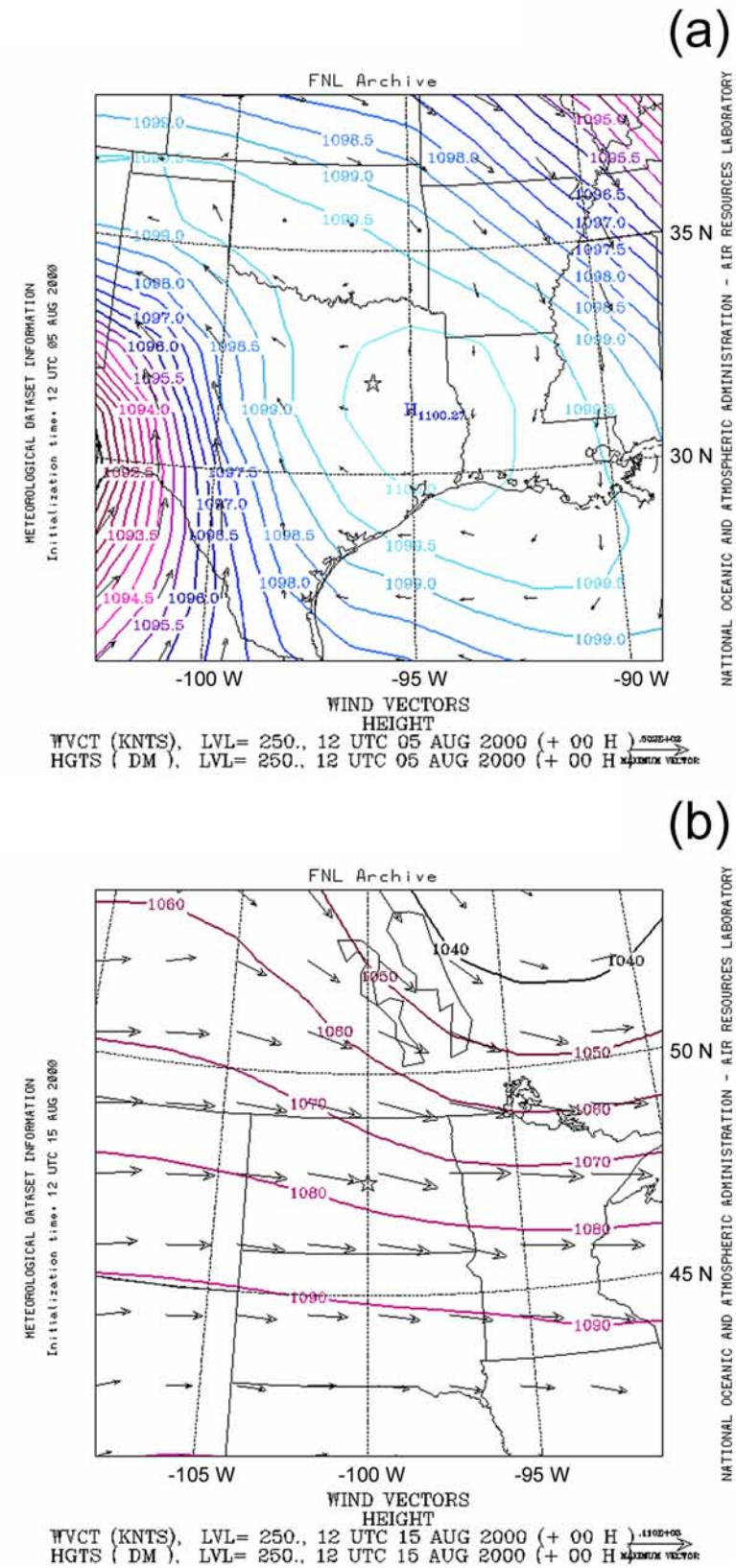

Figure 10. Geopotential height overlaid with wind fields at 250 hPa (a) for the Texas case at 1200 UTC on 5 August 2000 and (b) for the North Dakota case at 1200 UTC on 15 August 2000 with the FNL (the Global Final Analysis) archived meteorological data at NOAA Air Resources Laboratory (Real-Time Environment Applications and Display System (READY), http://www.arl.noaa.gov/ready.html).

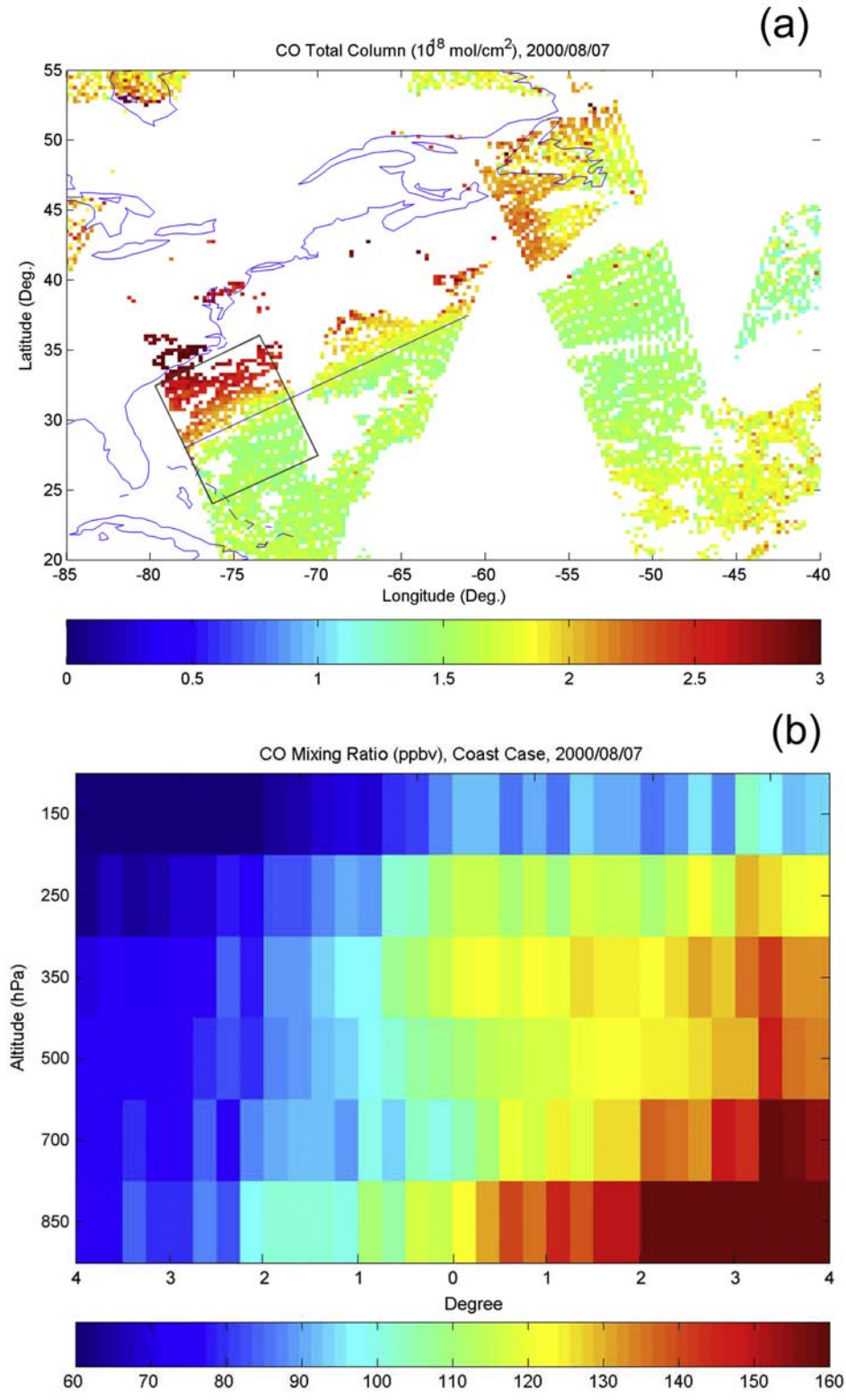

Figure 11. (a) CO total column (in 10^{18} molecules cm^{-2}) for the western Atlantic case on 7 August 2000. The location of the largest CO gradient is indicated with a line as a location reference. (b) Vertical cross section of the CO distribution for a nighttime pass (in the boxed area). The cross section is normal to the reference line in Figure 11a, extending ±4 degrees (=16 pixels) from the reference line. The mixing ratio values (in ppbv) represent the mean value within the boxed area in Figure 11a, averaged along the direction parallel to the reference line. Note that the vertical axis indicates the pressure levels for the MOPITT retrievals that are not evenly spaced. The surface CO is excluded because of low sensitivity of MOPITT to the CO in the boundary layer.

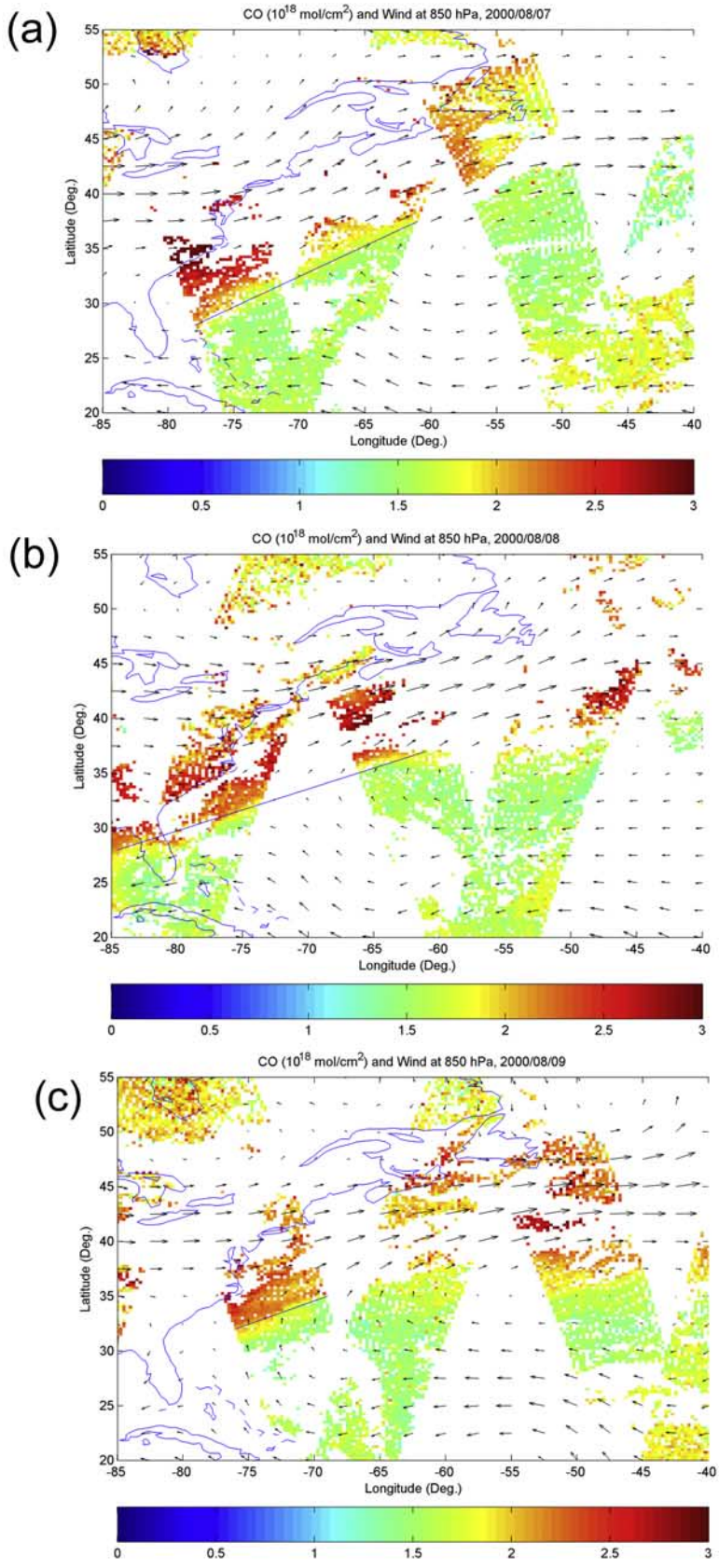

Figure 12. CO total column (in 10^{18} molecules cm^{-2}) on (a) 7 August 2000, (b) 8 August 2000, and (c) 9 August 2000 overlaid with the wind field at 850 hPa. The mean wind speed over the three images was 7.6 m s^{-1}. The location of large horizontal gradient of CO is indicated with a straight line for each day. The wind patterns from 1000 to 300 hPa were similar to those at 850 hPa.

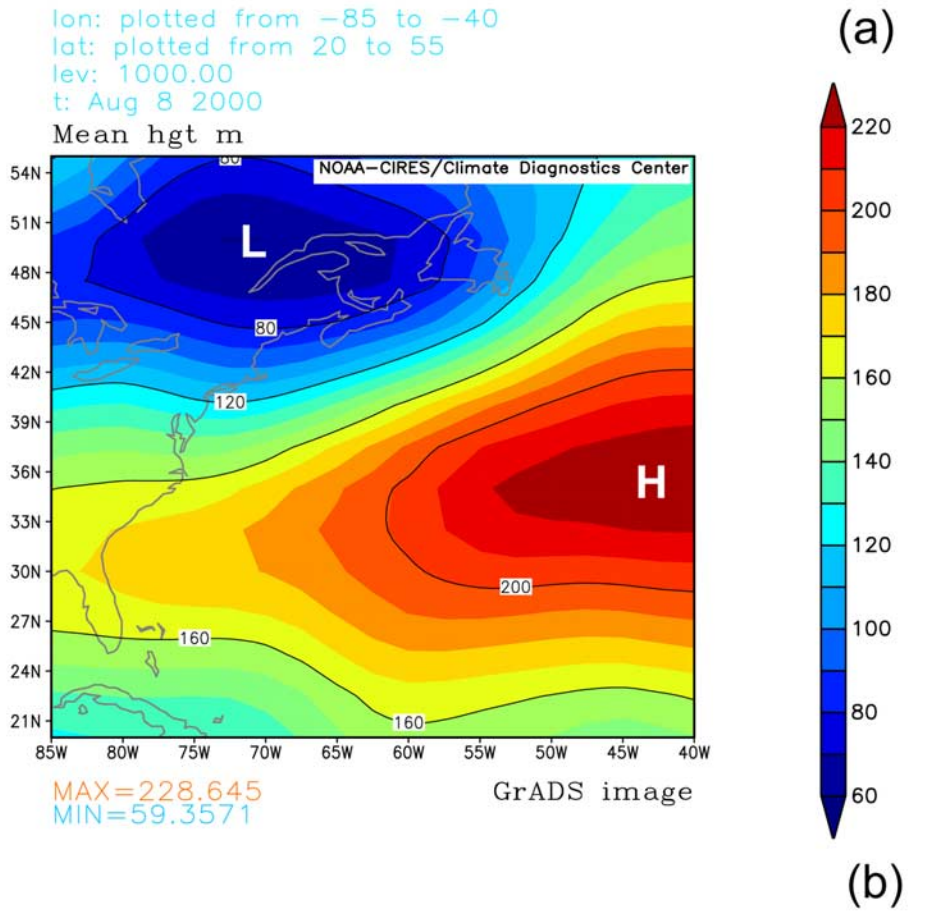

Figure 13. (a) Geopotential height (in meters) from NCEP Reanalysis data at 1000 hPa on 8 August 2000 for the Atlantic case. The center for the low-pressure system was around 49°N, 70°W, and the center for the high-pressure system was around 35°N, 40°W. (b) GOES-8 infrared image at 8 August 2000 at 0000 UTC.

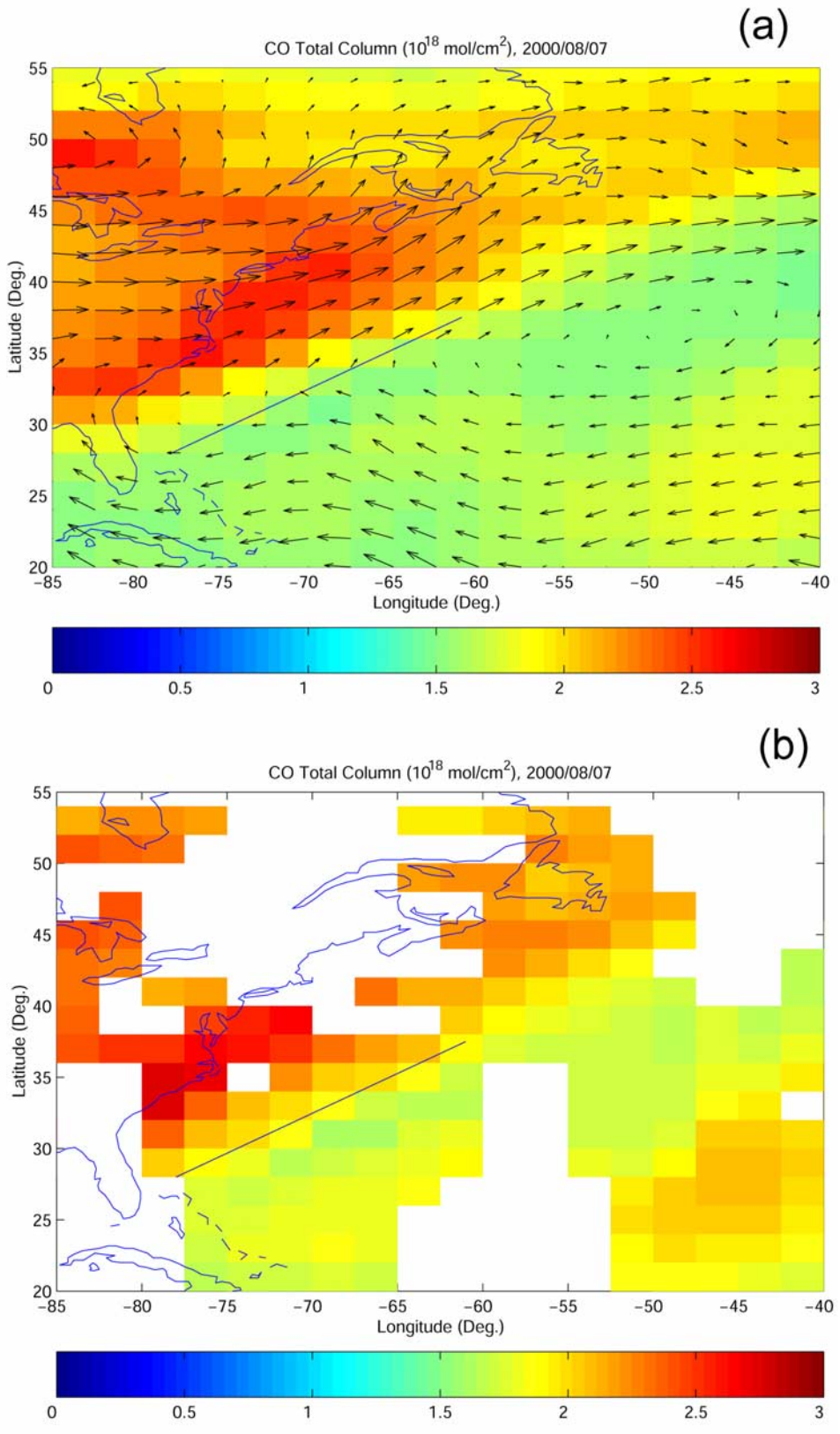

Figure 14. (a) CO total column (in 10^{18} molecules cm^{-2}) on 7 August 2000 as simulated by the GEOS-CHEM model. The modeled winds at the 850 hPa level are overlaid as arrows. The mean wind speed over the image was 7.7 m s^{-1}. (b) Modeled CO fields in Figure 14a after application of the local MOPITT averaging kernels. White areas indicate missing values due to clouds. The straight line indicates the location of the reference line in Figure 11a.

transport by WCBs and convection events. Using models alongside the data, we can now study the effects of these events on tropospheric chemistry.

[26] Through chemical processes, the concentration of CO in the troposphere is closely related to other gases, mostly OH and O_3 [*Jacob*, 1999]. It is also positively correlated to NO_y and SO_2 in the urban atmosphere, as found by *Wang et al.* [2003]. For these reasons, the variations in CO observed by MOPITTT could therefore provide a proxy for these pollutants. By integrating these data with chemical transport models and measurements of other trace gases at ground stations and by aircrafts and satellites, we can study the relationships between tropospheric CO and other trace gases in polluted regions.

[27] The MOPITT CO data can also be used for validation of three-dimensional global chemical transport models and regional air quality models. The good agreement of the GEOS-CHEM results with the MOPITT observations for Texas and Atlantic cases suggests that main processes controlling atmospheric CO are well presented in the model for these cases. However, the model cannot reproduce all the cases equally well, suggesting a need for model improvement.

[28] The MOPITT data have improved our understanding of the variation in CO associated with atmospheric dynamic processes. Before the MOPITT data became available, observations of this variation could only be made at surface stations and by aircrafts [*Bethan et al.*, 1998; *Chung et al.*, 1999; *Wang et al.*, 2003]. It is interesting that not all fronts identified in the weather charts are accompanied by CO discontinuities. This needs further investigation and may give clues to CO sources and transport mechanisms on regional scales. On the other hand, the information on CO variations offers opportunities to learn more about atmospheric dynamics because CO is a good tracer for diagnosing transport processes. For example, the vertical distribution of CO in a thunderstorm has its own characteristics because of deep convection and the associated dynamic processes [*Dickerson et al.*, 1987]. Therefore the MOPITT data can be useful in diagnosing the thunderstorm events, as well as the frontal systems shown in this study. The transport patterns of CO plumes from biomass burning in the tropics can provide an additional reference for simulating the wind fields in the region.

4. Conclusions

[29] We have examined the influence of synoptic processes on the distribution of CO as observed by the MOPITT satellite instrument. Analyzing the MOPITT data at a resolution close to their native spatial and temporal resolution, we observed large horizontal gradients in the CO distribution on synoptic scales, with total column abundances of CO varying by as much as 50–100% across distances of ~100 km. To determine the formation mechanisms responsible for the large gradients in the data, we selected three case studies from observations over North America in August 2000.

[30] In the first case, we observed that total CO columns over North Dakota on 15 August increased from $\sim 1.7 \times 10^{18}$ molecules cm^{-2} to $\sim 3.0 \times 10^{18}$ molecules cm^{-2} within a distance of less than 100 km, because of the passage of a cold front. The abundance of CO was enhanced ahead of the cold front as a result of the transport of air from Montana where there were large forest fires. Behind the cold front, clean air with low concentrations of CO was transported down from the Canadian Prairies.

[31] In the second case, we observed large horizontal gradients in CO, similar to the North Dakota case, over northeastern Texas on 5 August at all levels in the troposphere from 850 to 150 hPa. The total CO column abundance increased by a factor of approximately 1.5 within a distance of 150 km. Analysis of NCEP meteorological data and simulations from the GEOS-CHEM CTM suggest that the large gradients in CO reflected the influence of convective lifting of boundary layer air with high concentrations of CO over Arkansas, combined with the onshore transport of clean air from the Gulf of Mexico. In the model, advection and subsequent lofting by convection of CO produced by VOC oxidation over northern Louisiana and northeast Texas is mostly responsible for the high levels of CO.

[32] Finally, in the third case we focused on the continental export of pollution from the boundary layer along the east coast of North America by the WCBs associated with low-pressure systems in northeast Canada from 7 August to 9 August. The sharpest gradients were observed along the boundary between the WCB-transported polluted air and the clean air transported from the Atlantic by the semipermanent high-pressure system in the central Atlantic.

[33] Previous studies have assessed the ability of the MOPITT instrument to capture variations in the vertical structure of atmospheric CO associated with tropical deep convection and Asian summer monsoon [*Deeter et al.*, 2004; *Kar et al.*, 2004]. The findings presented here indicate that MOPITT can also capture the influence of synoptic processes on both the horizontal and vertical distribution of CO. This information may be lost when compositing the data at longer timescales and coarse spatial resolution. Recently, *Heald et al.* [2004] performed an inversion analysis of MOPITT data, averaged on a $2^\circ \times 2.5^\circ$ grid, and found differences in the estimates of the CO emissions from their inversion analysis depending on whether the data were employed at their native temporal resolution or averaged on weekly or monthly timescales.

[34] Atmospheric CO is a by-product of combustion, an important precursor of tropospheric O_3, and an ideal tracer of transport. The large gradients in CO observed on synoptic scales, therefore, represent valuable information that can be exploited to help improve our understanding of the pathways for export of pollution from the boundary layer to the free troposphere, and the interplay between transport and local sources and sinks of ozone precursors in determining regional air quality. The results presented here suggest that MOPTT observations provide a useful data set with which to address a range of issues from air quality on local/regional scales to long-range transport of pollutants on continental/global scales.

[35] **Acknowledgments.** The MOPITT project is funded by the Natural Sciences and Engineering Research Council (NSERC) of Canada, the Meteorological Service of Canada, and the Canadian Space Agency (CSA). The U.S. team and the Terra spacecraft are funded by NASA. We thank Anthony Liu and Clarck Zhao of University of Toronto for valuable

discussions. The GEOS-CHEM model is managed at Harvard University with support from the NASA ACMAP program.

References

Banic, C. M., G. A. Isaac, H. R. Cho, and J. V. Iribane (1986), The distribution of pollutants near a frontal surface: A comparison between field experiment and modeling, *Water Air Soil Pollut.*, *30*, 171–177.

Bethan, S., G. Vaughan, C. Gerbig, A. Volz-Thoms, H. Richer, and D. A. Tiddeman (1998), Chemical air mass differences near fronts, *J. Geophys. Res.*, *103*, 13,413–13,434.

Bey, I., D. J. Jacob, R. M. Yantosca, J. A. Logan, B. D. Field, A. M. Fiore, Q. Li, H. Y. Liu, L. J. Mickley, and M. G. Schultz (2001), Global modeling of tropospheric chemistry with assimilated meteorology: Model description and evaluation, *J. Geophys. Res.*, *106*, 23,073–23,095.

Brown, R. M., P. H. Daum, S. E. Schwartz, and M. R. Hjelmfelt (1984), Variations in the chemical composition of clouds during frontal passage, in *The Meteorology of Acid Deposition*, edited by P. J. Samson, pp. 202–212, Air Pollut. Control Assoc., Pittsburgh, Pa.

Chan, D., C. W. Yuen, K. Higuchi, A. Shashkov, J. Liu, J. Chen, and D. Worthy (2004), On the CO_2 exchange between the atmosphere and the biosphere: The role of synoptic and mesoscale processes, *Tellus, Ser. B*, *56*, 194–212.

Chung, K. K., J. C. L. Chan, C. N. Ng, K. S. Lam, and T. Wang (1999), Synoptic conditions associated with high carbon monoxide episodes at coastal station in Hong Kong, *Atmos. Environ.*, *33*, 3095–3099.

Daley, R. (1991), *Atmospheric Data Analysis*, Cambridge Univ. Press, New York.

Deeter, M. N., et al. (2003), Operational carbon monoxide retrieval algorithm and selected results for the MOPITT instrument, *J. Geophys. Res.*, *108*(D14), 4399, doi:10.1029/2002JD003186.

Deeter, M. N., L. K. Emmons, D. P. Edwards, J. C. Gille, and J. R. Drummond (2004), Vertical resolution and information content of CO profiles retrieved by MOPITT, *Geophys. Res. Lett.*, *31*, L15112, doi:10.1029/2004GL020235.

Dickerson, R. R., et al. (1987), Thunderstorms: An important mechanism in the transport of air pollutants, *Science*, *235*, 460–464.

Donnell, E. A., D. J. Fish, E. M. Dicks, and A. J. Thorpe (2001), Mechanisms for pollutant transport between the boundary layer and the free troposphere, *J. Geophys. Res.*, *106*, 7847–7856.

Drummond, J. R. (1992), Measurements of Pollution in the Troposphere (MOPITT), in *The Use of EOS for Studies of Atmospheric Physics*, edited by J. C. Gille and G. Visconti, pp. 77–101, Elsevier, New York.

Duncan, B. N., R. V. Martin, A. C. Staudt, R. Yevich, and J. A. Logan (2003), Interannual and seasonal variability of biomass burning emissions constrained by satellite observations, *J. Geophys. Res.*, *108*(D2), 4100, doi:10.1029/2002JD002378.

Edwards, D. P., C. M. Halvorson, and J. C. Gille (1999), Radiative transfer modeling for the EOS Terra satellite Measurement of Pollution in the Troposphere (MOPITT) instrument, *J. Geophys. Res.*, *104*, 16,755–16,775.

Emmons, L. K., et al. (2004), Validation of Measurements of Pollution in the Troposphere (MOPITT) CO retrievals with aircraft in situ profiles, *J. Geophys. Res.*, *109*, D03309, doi:10.1029/2003JD004101.

Evans, M. J., and D. J. Jacob (2005), Impact of new laboratory studies of N_2O_5 hydrolysis on global model budgets of tropospheric nitrogen oxides, ozone, and OH, *Geophys. Res. Lett.*, *32*, L09813, doi:10.1029/2005GL022469.

Fiore, A. M., D. J. Jacob, R. Mathur, and R. V. Martin (2003), Application of empirical orthogonal functions to evaluate ozone simulations with regional and global models, *J. Geophys. Res.*, *108*(D14), 4431, doi:10.1029/2002JD003151.

Fischer, H., et al. (2002), Synoptic tracer gradients in the upper troposphere over central Canada during the Stratosphere-Troposphere Experiments by Aircraft Measurements 1998 summer campaign, *J. Geophys. Res.*, *107*(D8), 4064, doi:10.1029/2000JD000312.

Heald, C. L., et al. (2003), Asian outflow and transpacific transport of carbon monoxide and ozone pollution: An integrated satellite, aircraft and model perspective, *J. Geophys. Res.*, *108*(D24), 4804, doi:10.1029/2003JD003507.

Heald, C. L., D. J. Jacob, D. B. A. Jones, P. I. Palmer, J. A. Logan, D. G. Streets, G. W. Sachse, J. C. Gille, R. N. Hoffman, and T. Nehrkorn (2004), Comparative inverse analysis of satellite (MOPITT) and aircraft (TRACE-P) observations to estimate Asian sources of carbon monoxide, *J. Geophys. Res.*, *109*, D23306, doi:10.1029/2004JD005185.

Jacob, D. (1999), *Introduction to Atmospheric Chemistry*, Princeton Univ. Press, Princeton, N. J.

Kar, J., et al. (2004), Evidence of vertical transport of carbon monoxide from Measurements of Pollution in the Troposphere (MOPITT), *Geophys. Res. Lett.*, *31*, L23105, doi:10.1029/2004GL021128.

Kowol-Santen, J., M. Beekmann, S. Schmitgen, and K. Dewey (2001), Tracer analysis of transport from the boundary layer to the free atmosphere, *Geophys. Res. Lett.*, *28*, 2907–2910.

Lamarque, J.-F., et al. (2003), Identification of CO plumes from MOPITT data: Application to the August 2000 Idaho-Montana forest fires, *Geophys. Res. Lett.*, *30*(13), 1688, doi:10.1029/2003GL017503.

Li, Q. B., D. J. Jacob, R. J. Park, Y. X. Wang, C. L. Heald, R. Hudman, R. M. Yantosca, R. V. Martin, and M. J. Evans (2005), North American pollution outflow and the trapping of convectively lifted pollution by upper-level anticyclone, *J. Geophys. Res.*, *110*, D10301, doi:10.1029/2004JD005039.

Liu, H. Y., D. J. Jacob, I. Bey, R. M. Yantosca, B. N. Duncan, and G. W. Sachse (2003), Transport pathways for Asian combustion outflow over the Pacific: Interannual and seasonal variations, *J. Geophys. Res.*, *108*(D20), 8786, doi:10.1029/2002JD003102.

Liu, J., J. R. Drummond, Q. Li, J. C. Gille, and D. C. Ziskin (2005), Satellite mapping of CO emission from forest fires in northwest America using MOPITT measurements, *Remote Sens. Environ.*, *95*, 502–516.

Palmer, P. I., D. J. Jacob, A. M. Fiore, R. V. Martin, K. Chance, and T. Kurosu (2003), Mapping isoprene emissions over North America using formaldehyde column observations from space, *J. Geophys. Res.*, *108*(D6), 4180, doi:10.1029/2002JD002153.

Pan, L., J. C. Gille, D. P. Edwards, P. L. Bailey, and C. D. Rodgers (1998), Retrieval of tropospheric carbon monoxide for the MOPITT experiment, *J. Geophys. Res.*, *103*, 32,277–32,290.

Park, R. J., D. J. Jacob, M. Chin, and R. V. Martin (2003), Sources of carbonaceous aerosols over the United States and implications for natural visibility, *J. Geophys. Res.*, *108*(D12), 4355, doi:10.1029/2002JD003190.

Rodgers, C. D. (2000), *Inverse Methods for Atmospheric Sounding: Theory and Practice*, World Sci., River Edge, N. J.

Stohl, A. (2001), A 1-year Lagrangian "climatology" of airstreams in the Northern Hemisphere troposphere and lowermost stratosphere, *J. Geophys. Res.*, *106*, 7263–7279.

Suntharalingam, P., D. J. Jacob, P. I. Palmer, J. A. Logan, R. M. Yantosca, Y. Xiao, M. J. Evans, D. Streets, S. A. Vay, and G. Sachse (2004), Improved quantification of Chinese carbon fluxes using CO_2/CO correlations in Asian outflow, *J. Geophys. Res.*, *109*, D18S18, doi:10.1029/2003JD004362.

Wang, T., C. N. Poon, Y. H. Kwok, and Y. S. Li (2003), Characterizing the temporal variability and emission patterns of pollution plumes in the Peal River Delta of China, *Atmos. Environ.*, *37*, 3539–3550.

Wang, Y. X., M. B. McElroy, D. J. Jacob, and R. M. Yantosca (2004), A nested grid formulation for chemical transport over Asia: Applications to CO, *J. Geophys. Res.*, *109*, D22307, doi:10.1029/2004JD005237.

Warner, J. X., J. C. Gille, D. P. Edwards, D. C. Ziskin, M. W. Smith, P. L. Bailey, and L. Rokke (2001), Cloud detection and clearing for the Earth Observing System Terra satellite Measurements of Pollution in the Troposphere (MOPITT) experiment, *Appl. Opt.*, *40*, 1269–1284.

Yevich, R., and J. A. Logan (2003), An assessment of biofuel use and burning of agricultural waste in the developing world, *Global Biogeochem. Cycles*, *17*(4), 1095, doi:10.1029/2002GB001952.

H. Bremer, Institute of Environmental Physics, University of Bremen, P. O. Box 330440, D-28334 Bremen, Germany.

Z. Cao, Meteorological Service of Canada–Ontario, 867 Lakeshore Road, Burlington, ON, Canada L7R 4A6.

J. R. Drummond, D. B. A. Jones, J. Kar, J. Liu, F. Nichitiu, and J. Zou, Atmospheric Science, Department of Physics, University of Toronto, 60 St. George Street, Toronto, ON, Canada M5S 1A7. (jliu@atmosp.physics.utoronto.ca)

J. C. Gille, National Center for Atmospheric Research, P. O. Box 3000, Boulder, CO 80307-300, USA.